Available online at www.sciencedirect.com

ScienceDirect

Energy Procedia 158 (2019) 1559–1564

Energy Procedia

www.elsevier.com/locate/procedia

10th International Conference on Applied Energy (ICAE2018), 22-25 August 2018, Hong Kong, China

Thermo-mechanical analysis of thermoelectric devices based on single p-n pair

Yue Tian [a], Zhuang Miao [a], Xiangning Meng [a] *, Wensheng Yan [b] *, Miaoyong Zhu [a]

[a] *School of Metallurgy, Northeastern University, Shenyang 110819, China*
[b] *Institute of Microstructure Technology, Karlsruhe Institute of Technology, Karlsruhe 76344, Germany*
**email: mengxn@mail.neu.edu.cn (corresponding author)*
**email: Wensheng.yan@kit.edu (corresponding author)*

Abstract

Thermoelectric devices have significant thermal stress and deformation affected by the temperature difference, which affecting their working stability and life span. In this paper, thermoelectric pairs are allocated in the *x*, *y* and *z* directions respectively to a single thermoelectric pair. And the maximum stress and deformation in all schemes are calculated by the finite element analysis. The results show that the interaction of the thermoelectric pairs in the *z* direction makes the maximum stress and the deformation decrease. The interaction of the *z*-direction thermoelectric pairs is beneficial to the reliability of thermoelectric devices. When designing thermoelectric devices, reducing the number of arrangement in the *x*, *y* directions and increasing the number of arrangement in the *z* direction can effectively improve their working stability and life span.

Keywords: thermoelectric device; thermoelectric pair; stress; deformation; finite element analysis

1. Introduction

Thermoelectric technology is a new method of directly converting the heat into electricity using Seebeck effect. It is in line with the trend of times. Thermoelectric devices are widely used in various fields, which can use industrial

* Corresponding author. Tel.: +86-24-83671706; fax: +86-24-83671706.
E-mail address: mengxn@mail.neu.edu.cn

10.1016/j.egypro.2019.01.366

waste heat, flue gas waste heat and some low-grade heat sources for power generation. It also can be used in solar power generation [1], aerospace [2], automotive waste heat recovery [3] and other fields. At present, researchers have achieved remarkable results in improving the efficiency of thermoelectric power generation from many aspects, such as thermoelectric materials, energy transmission characteristics, geometric parameters and so on [4-5]. Up to now, the stress and deformation distributions of various thermoelectric devices have been studied. So far, researchers have analyzed the mechanical properties of thermoelectric devices from the aspects of stress distribution, thermoelectric materials and geometrical parameters [6-8]. But the basic research on thermoelectric devices is still lacking. Therefore, this paper purposes with the basic single thermoelectric pairs and explores the influence of the interaction between thermoelectric pairs on the reliability of thermoelectric devices. First, the stress and deformation distributions of single thermoelectric pair are analysed. And then we construct three contrast schemes to analyze the stress and deformation variation of single thermoelectric pairs after allocating two thermoelectric pairs in three directions. Through analysis, which scheme is most favourable for the reliability of thermoelectric devices can be found.

2. Modeling

2.1. Model description

The main factor affecting the stability and life span of thermoelectric devices is the failure of the welding layer in the module. Stress is the main factor that destroys the weld layer. Factors of affecting stress include temperature and material properties. The physical parameters of each part of the thermoelectric modules are shown in **Table 1**.

Table 1 Physical parameters of each part of the thermoelectric devices [9].

	Coefficient of thermal expansion / K^{-1}	Elastic modulus / GPa	Poisson ratio	Coefficient of thermal conductivity / $W \cdot m^{-1} \cdot K^{-1}$
Al_2O_3 ceramics	0.65×10^{-5}	380	0.26	17
Copper sheet	1.8×10^{-5}	110	0.34	401
P-type semiconductor	1.68×10^{-5}	47	0.4	1.3
N-type semiconductor	1.68×10^{-5}	47	0.4	1.2

The thermoelectric pair is basic structure of a thermoelectric module, including insulators, copper sheets, and a p-n thermoelectric unit, as shown in **Fig 1 (a).** The thermoelectric unit is a cube with length of side a = 1 mm, spacing of thermoelectric units d = 0.5 mm, thickness of copper sheets m = 0.1 mm, thickness of insulator l = 0.5 mm.

Three contrast schemes are constructed, which are called scheme I, II and III. The central thermoelectric pairs of the three schemes are taken for analysis. Interface between insulator and copper interface at the hot end is the studied interface. Lines a and b on the interface are set as studied objects, which is shown in **Fig 1 (b)**. The cold end temperature of thermoelectric modules is 313 K and the hot end temperature is 333 K. In Scheme III, the cold end temperature is 293 K and the hot end temperature is 353 K to ensure that the central thermoelectric pair has same temperature difference. All interfaces are adiabatic except for the upper and lower surfaces.

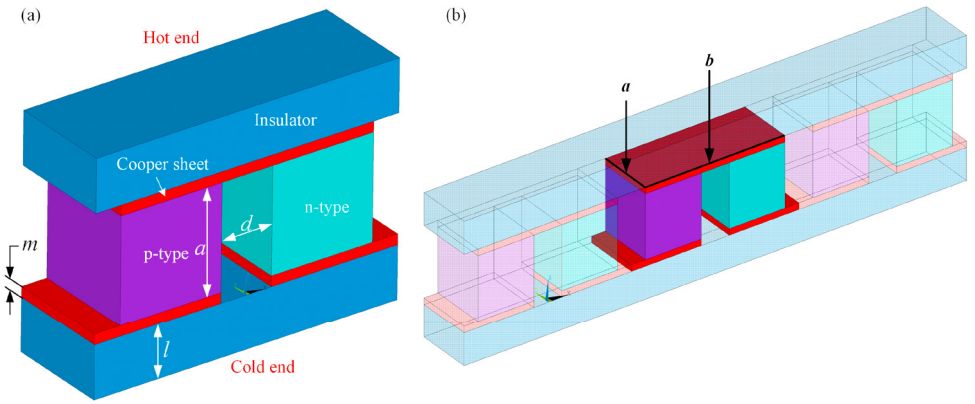

Fig. 1. Related research objects: **(a)** Diagram of the single thermoelectric pair; **(b)** model of Scheme I

2.2. Governing Equations

The heat conduction differential equation of three-dimensional steady state without internal heat source in Cartesian coordinate system is:

$$\frac{\partial}{\partial x}\left(\lambda\frac{\partial t}{\partial x}\right)+\frac{\partial}{\partial y}\left(\lambda\frac{\partial t}{\partial y}\right)+\frac{\partial}{\partial z}\left(\lambda\frac{\partial t}{\partial z}\right)=0 \tag{1}$$

Where, ρ is the density of an object, c is specific heat capacity, λ is the thermal conductivity, and T is the temperature at x.

The linear stress σ_x、σ_y、σ_z and shear stress τ_{xy}、τ_{yz}、τ_{zx} can be obtained from the coupled thermal-structural governing equations in three directions. From the fourth strength theory we can know:

$$\sigma_{r4}=\sqrt{\frac{1}{2}\left[\left(\sigma_x-\sigma_y\right)^2+\left(\sigma_y-\sigma_z\right)^2+\left(\sigma_z-\sigma_x\right)^2+6\left(\tau_{xy}^2+\tau_{yz}^2+\tau_{zx}^2\right)\right]}\le[\sigma] \tag{2}$$

σ_{r4} is the von mises stress. When σ_{r4} is less than the allowable stress [σ], the microelement is elastic deformation, and on the contrary, the microelement is plastic deformation.

3. Results and discussion

3.1. Stress-deformation analysis of single thermoelectric pair

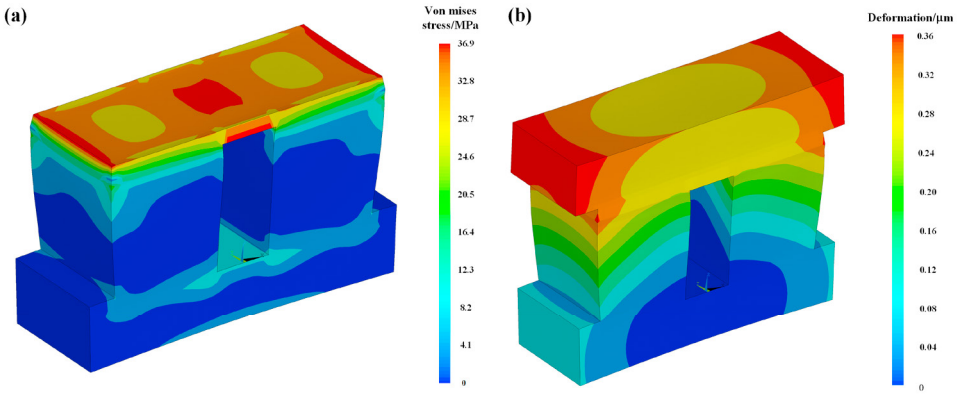

Fig. 2 Single thermoelectric pair: **(a)** Distribution of stress; **(b)** Distribution of deformation

Fig 2 (a) shows the equivalent stress diagram of a single thermoelectric pair. The stress concentration appears at the interface between insulator and copper sheet at the hot end. The maximum stress appears at the corner of the interface, and its value is about 36.741 MPa. **Fig 2 (b)** shows the deformation distribution of the single thermoelectric pair. The deformation distribution is regular and spherical around the central point. The maximum deformation appears at the edge of insulator with a value about 0.361 μm. The stress distributions of lines a and b are shown in **Fig 3**. The maximum stress appears at both ends of lines a and b. Because of the phenomenon of stress concentration at both ends, the local minimum value of 34.174 MPa appears at y = 0.05 mm and 0.95 mm on line a.

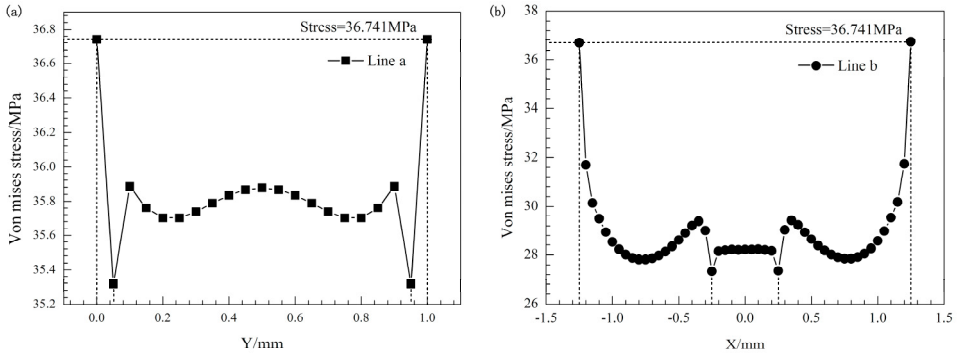

Fig. 3 The equivalent stress distribution: **(a)** Line a; **(b)** Line b

3.2. Analysis of x-direction thermoelectric pairs

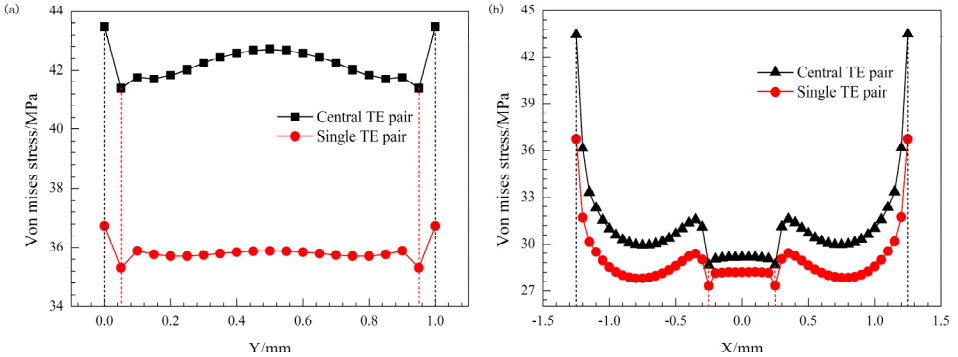

Fig. 4 Comparison of transverse modules: **(a)** Comparison of line a stress;**(b)** Comparison of line b stress.

Maximum stress of the central thermoelectric pair is about 43.471 MPa. The maximum deformation is about 0.336 μm. Stress comparison with the original single thermoelectric lines a and b is shown in **Fig 4**. The stress of line a increases obviously. Stress fluctuations still appear at y= 0.05 mm and 0.95 mm. Maximum increment of stress in middle area is about 1.314 MPa. Scheme I makes the stress at the studied interface increase and stress increment at both sides of the x-direction is larger.

3.3. Analysis of y-direction thermoelectric pairs

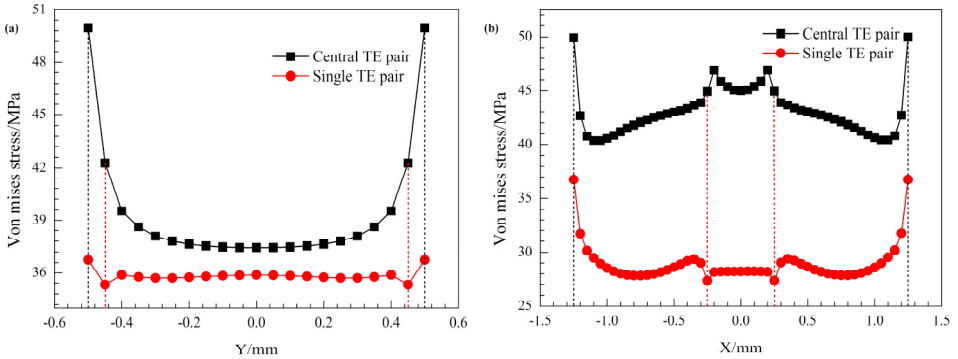

Fig. 5 The equivalent stress distribution: **(a)** Line a; **(b)** Line b

Maximum stress of the central thermoelectric pair is about 49.967 MPa. Maximum deformation is about 0.362

μm. **Fig 5** shows stress comparison of lines a and b with the original single thermoelectric pair. The stress on line a increases significantly. Maximum increment of stress is about 6.957 MPa except the maximum value points. It is much smaller than the maximum stress increment. In addition, the stress fluctuations at y = 0.05 mm and 0.95 mm disappear. The maximum increment is about 18.714 MPa in the middle area. In summary, the stress on the studied interface of the central thermoelectric pair increases. The increment of both sides in the *y* direction is larger, which leads to the disappearance of the stress fluctuation in the line a.

3.4. Analysis of z-direction thermoelectric pairs

The maximum stress of the central thermoelectric pair is about 36.126 MPa. The maximum deformation is about 0.332 μm. Stress comparison of lines a and b with the original single thermoelectric pair is shown in **Fig 6**. The stress reduction occurs at all points of line a. The maximum reduction is about 1.336 MPa. The stress on line b has the same properties and the stress is significantly reduced. The maximum reduction is about 2.247 MPa. Stress and deformation of the studied interface in the central thermoelectric pair decrease. It is beneficial to the stability of the central thermoelectric pair.

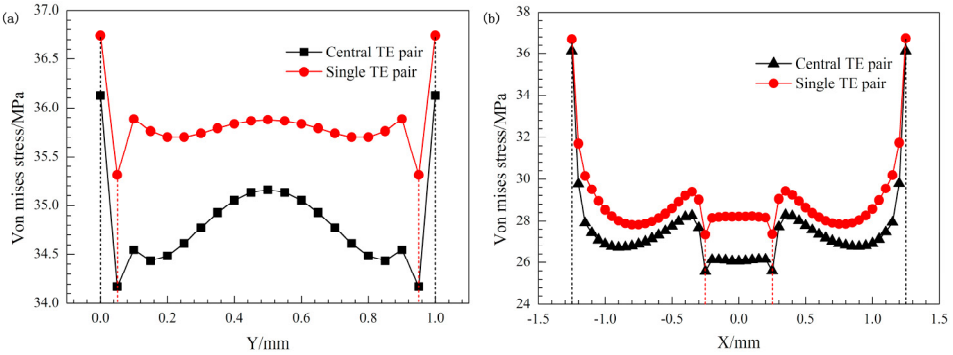

Fig. 6 The equivalent stress distribution: **(a)** Line a; **(b)** Line b

3.5. Comprehensive analysis

Overall analysis, in the central thermoelectric pair of Scheme I, the maximum stress increases and the maximum deformation decreases. In the central thermoelectric pair of scheme II, the maximum stress increases, and the increment is bigger than that of scheme I. The maximum deformation increases slightly. In the central thermoelectric pair of scheme III, both the maximum stress and the maximum deformation decrease. Scheme III is the best. Compared with scheme II, scheme I is a better solution. When designing the thermoelectric modules, the optimization sequence of allocating the thermoelectric pairs is $z > x > y$.

4. Conclusions

Through the numerical simulation of the thermal-structural coupling among the single thermoelectric pair and the three thermoelectric modules, the interaction of the thermoelectric pairs in *x*, *y* and *z* directions is analysed. And the following conclusions are obtained:

(1) The single thermoelectric pair is deformed by the temperature difference. The maximum stress of the single thermoelectric pair appears at the corners of the interface between the copper sheet and the insulator at the hot end. The maximum deformation appears at the edge of insulator.

(2) The interaction of *x*-direction thermoelectric pairs makes the deformation decrease and the stress increase. And the stress increases more significantly along both sides of the *x*-direction. The interaction of thermoelectric pairs in the *y*-direction makes the stress increase, which is more significant along both sides of the *y* direction. And the deformation increases slightly. The interaction of *z*-direction thermoelectric pairs makes the maximum stress and deformation decrease. Therefore, the scheme of allocating thermoelectric pairs in the *z* direction is the most advantageous.

Acknowledgements

Authors are grateful to financial supports from National Natural Science Foundation of China (51576034). Fundamental Research Funds for the Central Universities of China (N172502006), and Natural Science Foundation of Liaoning Province (201602258).

References

[1] T.T. Chow. A review on photovoltaic/thermal hybrid solar technology. Applied Energy, 2010, 87(2):365-379A.
[2] Zhiyong Huang, Zhifei Wu, Shixin Zhou, et al. Thermoelectric generator and in space and nuclear its application fields. Atomic Energy Science and Technology, 2004, 38(z1): 42-47.
[3] Lu H, Wu T, Bai S, et al. Experiment on thermal uniformity and pressure drop of exhaust heat exchanger for automotive thermoelectric generator. Energy, 2013, 54(54):372-377.
[4] Lu B, Meng X, Tian Y, et al. Thermoelectric performance using counter-flowing thermal fluids. International Journal of Hydrogen Energy, 2017.
[5] Meng X, Fujisaka T, Suzuki R O, et al. Thermoelectric analysis for helical power generation systems. Journal of Electronic Materials, 2014, 43(6):1509-1520.
[6] Ming T, Yang W, Wu Y, et al. Numerical analysis on the thermal behavior of a segmented thermoelectric generator. International Journal of Hydrogen Energy, 2016.
[7] Picard M, Turenne S, Vasilevskiy D, et al. Numerical simulation of performance and thermomechanical behavior of thermoelectric modules with segmented bismuth-telluride-based legs. Journal of Electronic Materials, 2013, 42(7):2343-2349.
[8] Soto M A, Venkatasubramanian R. ANSYS-based detailed thermo-mechanical modeling of complex thermoelectric power designs. International Conference on Thermoelectrics, IEEE, 2005:219-221.
[9] Fleurial J P, Johnson K, Mondt J, et al. Development of segmented thermoelectric multicouple converter technology. Aerospace Conference. IEEE, 2006:10 pp.